Fuel 265 (2020) 116949

Contents lists available at ScienceDirect

Fuel

journal homepage: www.elsevier.com/locate/fuel

Full Length Article

Experimental study on foamy oil flow behavior of a heavy oil-N_2 system under reservoir condition

Binyang Zou[a,b], Wanfen Pu[a,*], Xiao Hu[b], Xiang Zhou[a,b,*], Aiping Zheng[c], Fanhua Zeng[b,*]

[a] State Key Laboratory of Oil and Gas Reservoir Geology and Exploitation, Southwest Petroleum University, Chengdu, Sichuan 610500, PR China
[b] Petroleum Systems Engineering, Faculty of Engineering and Applied Science, University of Regina, Regina, Saskatchewan S4S 0A2, Canada
[c] Heavy Oil Company, Xinjiang Oil Field, CNPC, Karamay, Xinjiang 834000, PR China

ARTICLE INFO

Keywords:
Heavy oil
N_2 huff-n-puff
Flow behavior
Foamy oil

ABSTRACT

For heavy reservoirs, conventional oil recovery methods are polymer flooding and Steam-assisted Gravity Drainage (SAGD). Such methods are affected by various factors including reservoir thickness, formation heterogeneity, heat loss, and cost, especially in deep heavy oil reservoirs. In these deep reservoirs, their crude oil has a viscosity in the tens of thousands of centipoises at surface conditions, but only a few hundred centipoises at high temperature. There is sufficient mobility of crude oil making it possible for nitrogen (N_2) huff-n-puff to be applied. Since foamy oil is a very significant production mechanism in huff-n-puff process, this study is to confirm the ability of nitrogen to form foamy oil in a deep heavy oil reservoir.

This study includes two types of tests. The first category is the PVT tests to measure N_2 solubility in heavy oil. It was found that the solubility of nitrogen in the oil sample at 50 °C and 7 MPa is 7.54 m^3/m^3. The second category is the pressure depletion tests conducted in a 1-D cylindrical model to observe the flow behavior. These tests are conducted consistently at four different pressure decline rates. It confirmed the possibility of foamy oil formed by nitrogen and summarized the variation of the flow pattern.

This research is a preliminary basic study of N_2 huff-n-puff in heavy oil reservoirs. Confirmation of the technology's feasibility will significantly reduce the cost of exploiting heavy oil reservoir.

1. Introduction

Petroleum, although a nonrenewable energy source, will remain as the primary source of energy worldwide [23]. Unlike the increasing demand for oil, the scarcity of conventional oil reservoirs makes it a challenge to meet the demand. Fortunately, unconventional oil reservoirs account for 70% of total oil reserves worldwide [10]. Therefore, exploitation of unconventional oil reservoirs in the current oil industry has become the main focus to increase oil production [5,36,46].

Unconventional oil reservoirs are reservoirs with a wide variety of sources, which include oil sands, heavy oil, gas to liquids, tight oil, oil shale, and other liquids [36]. Among them, the recoverable reserves of tight oil and heavy oil are 47.0% and 29.7%, respectively. Tight oil and heavy oil are considered as the momentous resources for meeting the rapidly growing oil demand.

Heavy oil generally consists of oil sand, extra heavy oil or bitumen, which are trapped in unconsolidated sandstones. These types of crude oil are extremely viscous, making extraction difficult. Due to the high viscosity, heavy oil and bitumen are unable to be pumped out by conventional production methods. Compared with conventional reservoirs, there is more residual oil in unconventional reservoirs after primary recovery. Nevertheless, due to the unique properties of heavy oil and the unconsolidated sandstones, the conventional displacement method of restoring reservoir pressure utilizing water, natural gas or carbon dioxide injection has no functional effect [19]. Thermal recovery is currently the preferred method to exploit heavy oil reservoirs [40]. Thermal methods mostly refer to steam injection, which is the most effective method to reduce heavy oil viscosity.

However, for deep heavy oil reservoirs, due to the length of the wellbore being long, the heat loss becomes tremendous [9,12,40], causing a considerable amount of heating required [27]. In fact, many heavy oil resources are buried in relatively deep formations. For example, in China, most of the heavy oil reservoirs have a depth of more than 1000 m, and some even exceed 4000 m [6,11,31,33,34]. Since environmental issues become more prominent, the cost of carbon

* Corresponding authors at: State Key Laboratory of Oil and Gas Reservoir Geology and Exploitation, Southwest Petroleum University, Chengdu, Sichuan 610500, PR China (X. Zhou).
E-mail addresses: puwanfenswpu@163.com (W. Pu), zhouxiang@uregina.ca, zhou326x@gmail.com (X. Zhou), fanhua.zeng@uregina.ca (F. Zeng).

https://doi.org/10.1016/j.fuel.2019.116949
Received 24 July 2019; Received in revised form 30 October 2019; Accepted 22 December 2019

dioxide treatment continues to increase. Moreover, the international oil price is very low as of 2019. Under various factors, steam-based methods become uneconomical [8,50]. For such reservoirs, Many researchers have proposed that the gas/solvent-based method is more reasonable [16,25][35,47,48], and cyclic gas/solvent injection (huff-n-puff) is more efficient than continuous gas/solvent injection methods [44,49].

In the huff-n-puff process, fluids are first injected into a producer well, then the well is shut off for soaking, finally, the well is reopened for fluids to be produced. Natural gas or CO_2 is usually used as injection fluids in heavy oil reservoirs. Studies focusing on N_2 injection are relatively scarce in literature. N_2 is relatively difficult to dissolve in crude oil, and has higher miscible pressure. Therefore, the effect of N_2 injection is generally not as good as that of the CO_2 or natural gas [17]. However, when the reservoir is relatively deep, the formation temperature is relatively high. The advantage of this reservoir condition is that even if the crude oil viscosity underground is high, the crude oil can maintain sufficient mobility under such high temperature. This makes it unnecessary to use expensive hydrocarbon or CO_2 gases in the huff-n-puff method. Nitrogen, on the other hand, can meet the demand and further reduce costs. It also has low solubility in water and is difficult to react with formation fluids and rock minerals. It can avoid emulsification, sedimentation, blockage of the formation, and corrosion of the ground/underground equipment. Nitrogen does not support combustion, it is not explosive, and it is safe and reliable. Nitrogen has been widely and successfully used as the injection gas for EOR in oil field operations [13,28,32,38]. It is an ideal gas for gas cycling, reservoir pressure maintenance, lifting and driving oil flow. Combing the use of advanced membrane separation nitrogen production technology [3,4,20] with inexhaustible air resources, it is possible to efficiently and quickly produce large amount of nitrogen with a purity of more than 95% directly into the well. Therefore, when the cost is low, the source is widespread, and the construction is convenient, nitrogen has the potential to become the comprehensive and large-scale popularization of application technology.

N_2 huff-n-puff application to unconventional reservoirs has been investigated by lots of researchers recently. Yue et al. used a three-dimensional (3D) quantitative sculpture geological model and the dynamic production analysis to study N_2 huff-n-puff process, and understand the mechanism of non-miscible N_2 injection are WOC adjustment and formation energy supplement in a fracture-vuggy type reservoir [43]. Meanwhile, Li et al. pointed out that three drive modes appear during huff-n-puff process in shale oil are gas cap drive, dissolved gas drive, and miscible drive [14]. Miller et al. compared the performance of Carbon Dioxide/Nitrogen/Natural gas in oilfield tests. The N_2/CO_2 showed a higher recovery efficiency than the rich gas [22]. Nguyen et al. conduct direct visualization experiments with a microfluidic system to study the huff-n-puff methods in shale fracture networks, and proposed that bubble nucleation, growth, coalescence, and connected gas flow are the main mechanisms for the fracture networks [24]. Bai et al. found that in the process of N_2 huff-n-puff for tight oil reservoirs, the elasticity energy is dominant and fracture arrangement in space hardly to improve oil recovery [2]. The experimental results of Yu et al. show that the pressure depletion rate, soaking time and the production time played important roles during the huff-n-puff gas injection process [42].

Previous research has focused on the application of N_2 huff-n-puff in shale or tight oil reservoirs. Research on nitrogen huff-n-puff process for heavy oil reservoirs has not been found in present published studies. Compared with the huff-n-puff process in light oil reservoirs, the most important mechanism of gas/solvent huff-n-puff in heavy oils is foamy oil flow [51]. Foamy oil flow refers to a unique two-phase flow, unlike normal two-phase flow, which requires a fluid phase to become continuous before it can flow, it involves flow of dispersed gas bubbles [18]. Since there is large capillary force due to the high viscosity of the heavy oil, these bubbles are trapped in the heavy oil. The evolved gas below the bubble point pressure forms bubbles that are carried with the flowing oil phase [29]. Most of the evolved gas remains in the form of dispersed gas in the oil phase, and does not form a continuous free gas phase, so this flow state is called “foamy oil” flow.

The main objective of this paper is to confirm nitrogen’s ability to form foamy oil flow and summarized the variation of the flow pattern. Since huff-n-puff process is affected by many other operating parameters, such as injection rate and time, number of cycles, soaking time, and pressure. These factors have been discussed in detail in previous studies [1,15,17,41,43]. In this paper, we focus on gas expansion and exsolution processes and mainly discuss the flow behavior of nitrogen-saturated heavy oil during pressure depletion process. The two experimental studies including PVT tests, and 1-D sand-pack tests. In PVT tests, the experiments are conducted in a mercury-free DBR Pressure-Volume-Temperature (PVT) system to measure the solubility of nitrogen in the heavy oil system. In the 1-D cylindrical sand-pack tests, pressure depletion tests are conducted on the heavy oil-nitrogen systems to determine the oil production curves under different constant pressure decline rates.

2. Experimental materials and method

2.1. Materials

The oil sample used in these experiments is a conventional heavy oil with a density of 0.98 g/cm^3. This oil sample can be regarded as dead oil because it is exposed to room temperature and pressure for a long time. This heavy oil sample is first settled to centrifuge at 3000 rpm for 90 min to make sure the dead oil sample is free of water. After the dehydration process, the viscosity of the dead oil is measured to be 6400 cP at 20 °C, and 598 cP at 50 °C. The viscosity of the heavy oil at different temperatures are shown in Table 1 and Fig. 1.

Water wet glass beads with an average diameter of 90–150 μm are used in packing the physical 1-D sandpack model. This model has a length of 95 cm and a diameter of 3.8 cm. The parameters of the dead oil and the 1-D cylindrical sand-pack model are shown in Table 2. Nitrogen gas sample is supplied by Praxair Canada Inc. The purity of nitrogen in the tank is higher than 99%, and the pressure of nitrogen is higher than 14 MPa.

2.2. PVT tests

2.2.1. Experimental setup

The PVT tests are conducted in a mercury-free DBR Pressure-Volume-Temperature (PVT) system. This system is divided into three sections as shown in Fig. 2.

1. Section A is the record and display system. It has a

Table 1
Viscosity of the Dead Oil Sample.

Temperature, °C	Experimental Data Viscosity, cP	Trend Line Viscosity, cP
19.2	6400	6408
25	4810	4100
29.7	2622	2855
30.1	2514	2769
39.5	1622	1342
40	1560	1292
40.4	1490	1253
41.5	1200	1151
43	870	1025
45	730	879
47.3	634	736
50	600	598
60	330	276

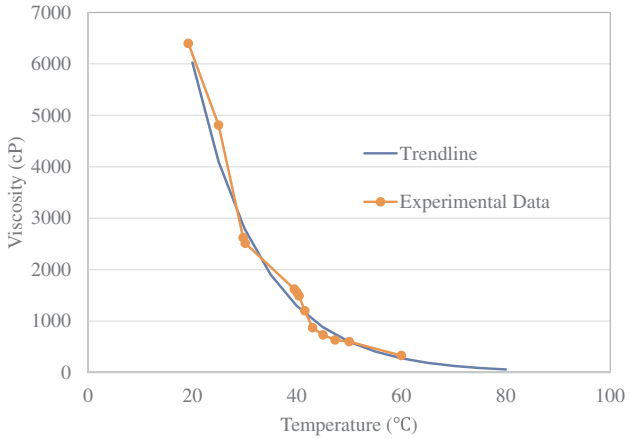

Fig. 1. Viscosity of the Dead Oil Sample.

Table 2
Parameters of the 1-D Cylindrical Sand-pack Model.

Parameter	Value
Diameter, cm	3.80
Cross-sectional Area, cm^2	11.34
Length, cm	95.00
Bulk Volume, cm^3	1077.41
Pore Volume, cm^3	377.00
Porosity, %	34.99
Permeability, Darcy	6.32
Initial Oil Saturation, %	93
Initial Water Saturation, %	7

high definition camera (as shown in Fig. 2.a), a camera lift controller (as shown in Fig. 2.b), and a display screen (as shown in Fig. 2.c).

2. Section B is the PVT cell and control system. It contains a visual PVT cell in an air bath (as shown in Fig. 2.), a control panel (as shown in Fig. 2.c) that regulates the temperature in the air bath, the magnetic stirrer in the PVT cell, and displays the pressure in the PVT cell.
3. Section C is the injection system. It contains two transfer cylinders with nitrogen and oil sample respectively, a vacuum pump, and a syringe pump.

2.2.2. *Experimental procedure*

The procedure of the PVT test involves following steps:

(1) PVT cell cleaning: To start the cleaning process, toluene, kerosene and ethanol are sequentially used to clean the PVT cell, and air is pump into the cell to dry the sand pack. At this stage, no more impurities existed in the PVT cell.

(2) Oil and Gas Injection: The injection volume of the oil sample is set to 20 ml, and correspondingly, nitrogen volume is set to be 1,500 ml at room temperature and pressure.

(3) Measurement: Since the conditions of the later experiments are at 7 MPa and 50 °C, a series of experiments are conducted to measure solubility at this pressure and temperature setting [39]. Increasing the pressure and temperature in the PVT cell to 7 MPa and 50 °C respectively, this state is maintained for 4 h while keeping the magnetic stirrer on. The function of the magnetic stirrer is to evenly dissolve nitrogen into the oil sample. When the piston height shows almost no change and pressure keeps stable or change slightly after 4 h, which means the heavy oil is saturated with N_2 at certain temperature and pressure, record the changes in piston height, real-time temperature, and real-time pressure. With the recorded measurements, calculate the solubility at this condition. Next, repeat the above steps to calculate the solubility at different pressure and temperature conditions. When the pressure is

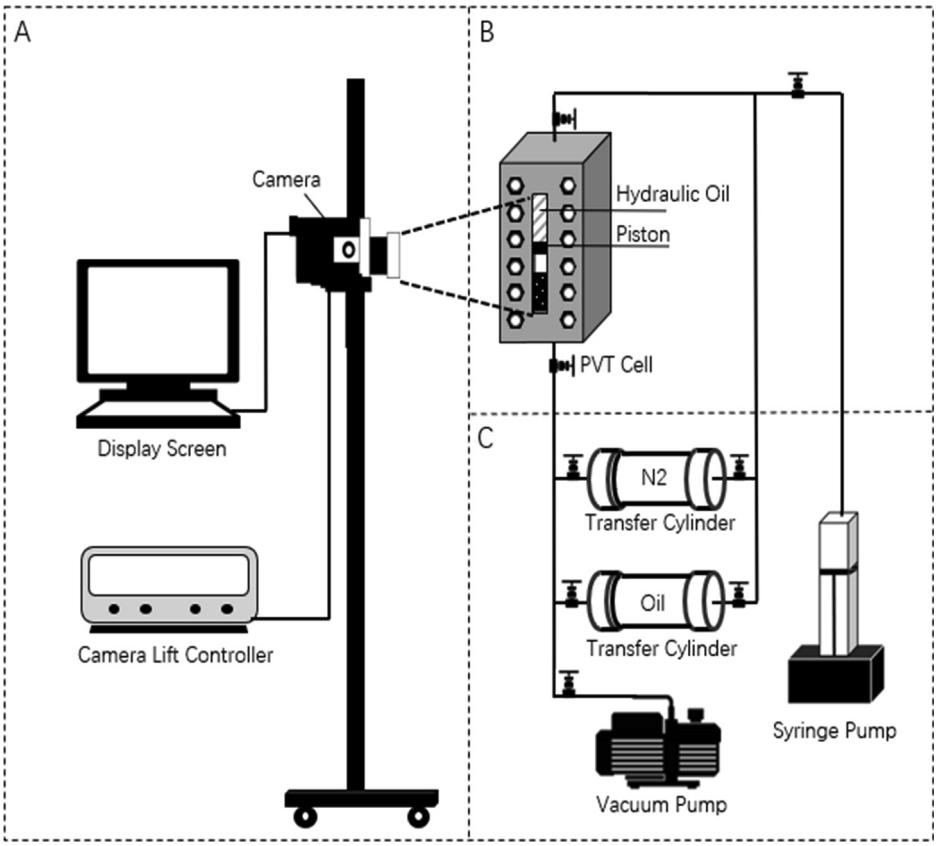

Fig. 2. DBR PVT System Schematic Plan.

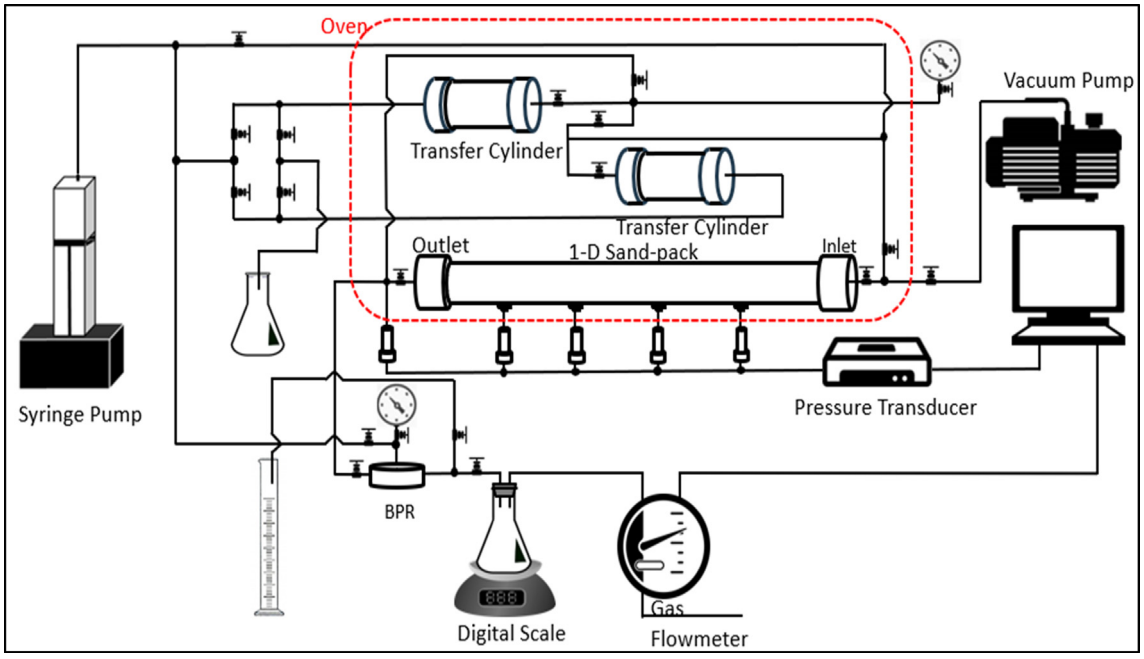

Fig. 3. Illustration of the Experimental Device System.

maintained at 7 MPa, the temperature is set from 40 to 80 °C with 5 °C incremental increase. Then the temperature is maintained at 55 °C, and the pressure is set from 7 to 1 MPa with 1 MPa incremental decrease.

2.3. Pressure depletion tests

2.3.1. Experimental setup

The illustration of the experimental device set-up is shown in Fig. 3. Two transfer cylinders are connected to the inlet end of the model. These two transfer cylinders are filled with gaseous nitrogen and live oil, respectively. The inner pressure or the flow rates of these two cylinders are controlled by a syringe pump. Both of the two transfer cylinders and the 1-D model are placed in an oven. The temperature of the oven is set at 50 °C to simulate the high-temperature formation environment. One back pressure regulator (BPR) is connected to the outlet end of the model, and its role is to control the pressure at the outlet. The syringe pump regulates the pressure of BPR. The outlet end of the BPR is connected to a production system, which consists of a digital scale and a gas flowmeter. This production system is used to measure oil production and gas production. The pressure transducers and the gas flow meter are all directly connected to the computer to record the readings automatically. The digital scale readings are recorded by the camera.

2.3.2. Experimental procedure

Pressure depletion tests include following steps:

(1) Live oil preparation: The process of preparing the live oil is to inject a certain proportion of dead oil and nitrogen into the same transfer cylinder while maintaining high pressure. The transfer cylinder is then fixed on a rotating machine for two days. The tation process is to ensure full contact between nitrogen and the dead oil until nitrogen is completely dissolved in the oil. In the pressure depletion experiments, it is assumed that the initial conditions of the reservoir are at 50 °C and 7 MPa. In order to ensure single-phase flow in the first stage of the experiments, the saturation pressure of the prepared live oil must be less than 7 MPa. It is required to prepare a live oil with a saturation pressure of 6 MPa at 50 °C.
(2) Sand-pack model preparation: Pour the glass beads into the model at a very slow rate while adjusting the vibrator to the maximum frequency. Ensure the sand fills the model evenly and tightly. After setting up the experimental system, nitrogen is injected into the model to increase the pressure to 7.5 MPa. If the pressure drop is less than 5 kPa in 24 h, the whole system is considered to be sealed. After that, the whole experimental system in pressure depletion tests is considered as a leak-free system. The pore volume of the model is measured by injecting water into the model, and once the water fills the entire pore space, the amount of water injected is equal to the pore volume. The absolute permeability is calculated by Darcy's law. A fixed flow rate is set to allow water to flow through the model. Once the pressure stabilizes at the inlet and outlet ends (this process usually lasts 5 min), the flow rate on the pump and the pressure readings at both ends are recorded. The flow rate is set from 2 to 20 ml/min with 2 ml/min incremental increase. After the above process, live oil is injected into the sandpack under a low flow rate. In these tests, the flow rate of 0.03 ml/min is selected. The live oil volume needed for injection is 1.5 times of the pore volume (PV) to ensure the model is well saturated with live oil [51]. After the sand-pack model is saturated with live oil, live oil is continuously injected into the model. Using Darcy's law to calculate the live oil viscosity. A fixed flow rate is set to allow live oil to flow through the model. Once the pressure at the inlet and outlet ends stabilizes (this process usually lasts for about 10 min), the flow rate on the pump and the pressure readings at both ends are recorded. The flow rate is set from 2 to 20 ml/min with 2 ml/min incremental increase.
(3) Test procedure: In this step, except for the inlet port, all other ports are opened. The initial pressure inside the model is set to 7 MPa, and so is the pressure of the BPR. Oil is produced with depletion back pressure under different constant pressure decline rates, which is controlled by the syringe pump. The outlet end of the BPR is connected to a production system, which consists of a digital scale and a gas flowmeter. This production system is used to measure oil production and gas production. In Zhou's study [51], the best pressure decline rate in terms of oil recovery factor and gas recovery for heavy oil-methane, heavy oil-propane and heavy oil-mixture gas system is 2 kPa/min. Therefore, the pressure decline rates in these tests start from 2 kPa/min to verify whether the heavy

Table 3
Solubility of Nitrogen at 7 MPa.

Pressure, kPa	Temperature, °C	Experimental Data	Trend Line
		Solubility, cm^3/cm^3	Solubility, cm^3/cm^3
7000	40.2	8.34	8.22
	44.9	7.98	7.90
	50.2	7.23	7.54
	55.4	7.32	7.18
	60.0	6.92	6.87
	64.9	6.44	6.54
	64.7	6.32	6.55
	70.0	6.40	6.19
	78.5	5.78	5.61
	80.5	5.36	5.47

oil-nitrogen system can form foamy oil or not. Then the pressure decline rate is changed to find the best condition to form the foamy oil.

3. Results and discussions

3.1. PVT tests

The first set of data is measured when the pressure is stable at 7 MPa, and the temperature is varied from 40 to 80 °C with 5 °C incremental increase. The result is shown in Table 3 and Fig. 4. From Fig. 4, it can be seen that when the pressure is constant, the solubility of nitrogen decreases linearly with increasing temperature.

For the second set of the experiments, the temperature is maintained at 50 °C, and the pressure is set from 7 to 1 MPa with 1 MPa incremental decrease. The result is shown in Table 4 and Fig. 5. It can be seen in Fig. 5 that when the temperature is constant, the solubility of nitrogen increases linearly as well with increasing pressure. The experimental data only has a solubility at 6.5 MPa, which is about 7.2 cm^3/cm^3.

Many researchers have measured the solubility of gases commonly used in CSI. Since the heavy oils used in other experiments are different, the experimental results cannot be directly compared. According to Mehrotra's research results, as shown in Table 5, the solubility of carbon dioxide is much higher than the solubility of methane and nitrogen. Although the solubility of nitrogen and methane differs slightly, the solubility of nitrogen is still only about one-half of that of methane. In summary, the solubility of nitrogen in heavy oil is less than that of carbon dioxide and methane.

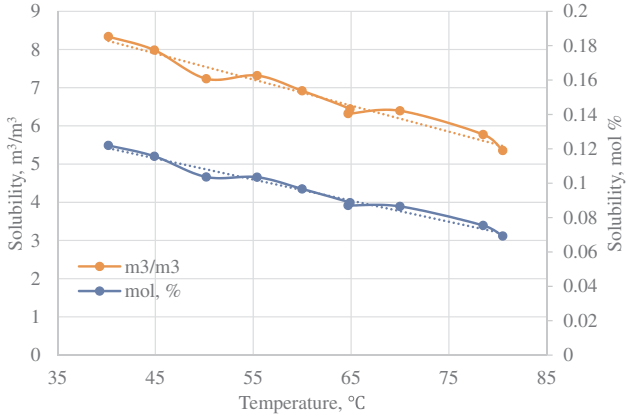

Fig. 4. Solubility of Nitrogen at 7 MPa.

Table 4
Solubility of Nitrogen at 50 °C.

Temperature, °C	Pressure, kPa	Experimental Data	Trendline
		Solubility, cm^3/cm^3	Solubility, cm^3/cm^3
50	7164	7.41	7.74
	6212	6.76	6.97
	5206	5.76	6.15
	4144	5.11	5.29
	3137	4.19	4.48
	2096	3.87	3.63
	1172	2.61	2.89

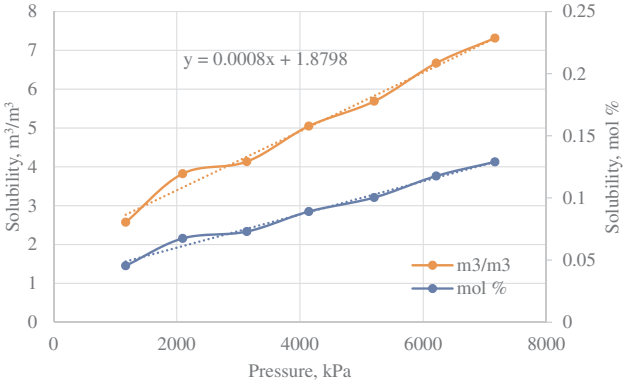

Fig. 5. Solubility of Nitrogen at 50 °C.

Table 5
Solubility comparison.

Temperature, °C	Pressure, MPa	Solubility, m^3/m^3			
		CO_2 [21]	CH_4 [21]	N_2 [21]	N_2 (in this study)
40	6	37.12	–		7.31
62	6	28.03	–		5.91
96.8	6	17.95	–		3.82
45	7	–	12.87		7.90
67	7	–	11.46		6.39
100	7	–	10.38		4.14
53.4	8.7			3.82	8.74
52.7	5.9			3.13	6.28
74.7	5.9			2.88	5.58

3.2. Pressure depletion tests

The oil recovery factor of the four experiments in these tests is listed in Table 6. Fig. 6 shows the cumulative oil production of the four pressure decline rate as a function of the dimensionless time, which is defined as T/Tt. Tt is the total experimental production time of each pressure decline rate. Based on the oil recovery and gas recovery data, it can be concluded that the higher the pressure decline rate, the greater the oil recovery factor.

3.2.1. Oil/gas production

The oil production performance behaves differently in all four experiments. Based on the shapes of the oil production curves in Fig. 6, the four sets of experiments can be divided into two groups. Pressure decline rates of 2 and 8 kPa/min are grouped together, and pressure decline rate of 16 and 32 kPa/min are grouped together. In the experiments of 2 and 8 kPa/min, there is no oil production at the beginning of the experiments, and oil production stays as low as zero. Then, the oil production rates start to increase at the end of the beginning period. During this period, oil production rate is relatively

Table 6
Oil/Gas Recovery Factor.

Sandpack Initial Pressure, kPa	Pressure Decline Rate, kPa/min	Cumulative Oil Production, g	Cumulative Gas Production, cm^3	Oil Recovery Factor, %	Gas Recovery Factor, %	Cumulative Gas/Oil Ratio, m^3/m^3
7000	2	46.8	2042.5	12.88	91.97	42.84
7000	8	61.4	1915	16.9	86.23	30.62
7000	16	90.6	1665	24.94	74.97	18.04
7000	32	117.6	1465	32.37	65.97	12.23

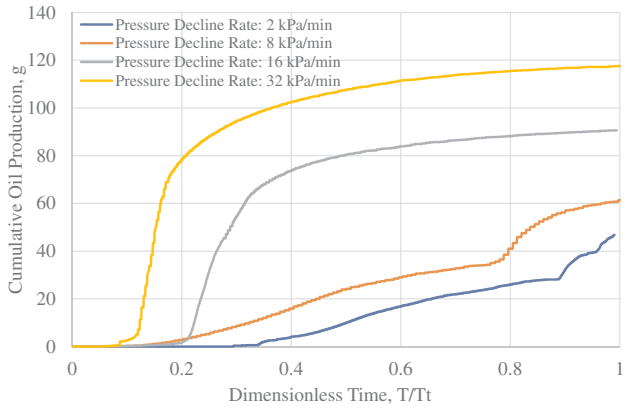

Fig. 6. Cumulative Oil Production.

stable. After these regions, there is a rapid increase in oil production until the end of these two experiments. In the latter two experiments with pressure decline rates of 16 and 32 kPa/min, there is also no oil production at the beginning. However, this is followed by a period of high-rate production. In this production period, oil production performs like foamy oil flow behavior where the oil production rate is maintained at a very high speed. After that, the oil production rate slowly decreases with time until approaching zero at the end of the experiments.

3.2.1.1. Pressure decline rate: 2 kPa/min. Fig. 7 is the cumulative oil production curve and the inner pressure curves as a function of time elapsed in the experiment with the pressure decline rate of 2 kPa/min. In the first 1,000 min, no oil is produced in this region. The reason for this phenomenon is that during this period, the inner pressure of the model is high than bubble point pressure (6000 kPa). Since nitrogen has not been released from the crude oil during this process, the fluid in the model remains as a single-phase flow. The driven force of the fluid is mainly derived from the elastic expansion of the saturated live oil. However, the volume expansion of crude oil is very small. The volumetric expansion of crude oil is negligible compared to the internal volume of the 1-D sand-pack model and the empty volume in the production tube. Therefore, in the first period of this region, no oil is produced from the sand-pack model. This production stage is considered as oil single-phase flow region [51]. Then, gas starts to produce, but there is still no oil production. In this period, the pressure in the model is lower than the bubble point pressure, and nitrogen begins to be released from the oil. However, because of the slow pressure decline rate, the solution gas drive is not enough to displace the oil. At this stage, there is only gas production and no oil production. So, this stage is considered to be a gas single-phase flow region. These two stages together are considered as the single-phase flow region.

When the outlet port pressure is less than 5,500 kPa, oil begins to be produced from the model. For a long time after this, the rate of oil production remains at a relatively stable level. The cumulative oil production curve of this stage changes relatively slowly. This production curve is very similar to the curve from the normal solution gas drive flow [26,30,37]. Since the experiment is conducted at a high temperature of 50 °C, the viscosity of the live oil is only 575 cP, and the pressure decline rate is very slow. Under this condition, the aggregation rate of small bubbles is much faster than the rate of generation of small bubbles, so the evolved gas forms a continuous free gas phase in a short time. At this stage, the flow state is dominated by normal gas/oil two-phase flow, and the main energy to produce is the expansion of continuous free gas. Consequently, this stage is considered as a normal solution gas drive region.

When this experiment runs to 53 h, and the pressure drops to about 400 kPa, there is a sudden increase in oil production rate. In this region, since the bubble generation rate increases, small bubbles begin to aggregate toward the nucleated bubbles and form a slightly larger bubble before they are separated from the oil. Because of the large volume of gas bubbles, oil–gas foamy flow volume is expanded rapidly. The evolved gas below the bubble point pressure forms bubbles that are carried with the flowing oil phase [29]. Unlike the gas/oil two-phase flow in the normal solution gas drive, most of the evolved gas remains in the form of dispersed gas in the oil phase, and does not form a continuous free gas phase, so this flow state is called “foamy oil” flow. Since oil production is mainly derived from foamy oil flow in this region, it is considered to be the foamy oil flow region. Many researchers found similar curve feature in their studies [37,45]. Zhang didn’t explain the reason, and Ming believes that this is due to the fact that after the gas is released from the oil, the viscosity of the oil rises sharply, causing the gas to be trapped in the oil to form a foamy oil. However, it was determined that the viscosity of the nitrogen-saturated live oil is only 25 cP lower than the viscosity of the dead oil at 50 °C. Therefore, it is unreasonable to attribute the increase in foamy oil to the increase in viscosity of crude oil. Rather, the most likely reason is that the bubbles released from the oil become larger and larger as the pressure decreases. After reaching a certain level, the flow of foamy oil suddenly increased.

3.2.1.2. Pressure decline rate: 8 kPa/min. When the pressure decline rate is 8 kPa/min, the single-phase flow region becomes narrower. Under this pressure decline rate, gas single-phase flow stage does not exist. The release rate of nitrogen is fast enough that the solution gas drive is sufficient to displace the oil. This pressure decline rate allows the normal solution gas drive region to begin directly after the oil single-phase flow region.

In the normal solution gas drive region, the oil production rate first rises slowly, and then drops slowly after reaching the apex, as shown in Fig. 8. The gas production rate has been rising steadily. This form of oil production and gas production is the same as the trend when the pressure decline rate is 2 kPa/min. The normal solution gas drive region of the two experiments with pressure decline rates of 2 and 8 kPa/min have the same slope in Fig. 6. Since the abscissa is dimensionless time, the same slope indicates that the average oil production per unit pressure depletion is the same which is approximately 0.00625 g/kPa (6.25 kg/ MPa). In other words, even if the pressure decline rate is increased by 4 times, the oil production per unit pressure depletion will not increase, but the gas production will increase significantly. This shows that there is an upper limit to the ability of normal solution gas drive to displace heavy oil. After reaching the upper limit, the increase in pressure decline rate will only increase gas production. Thus, in the

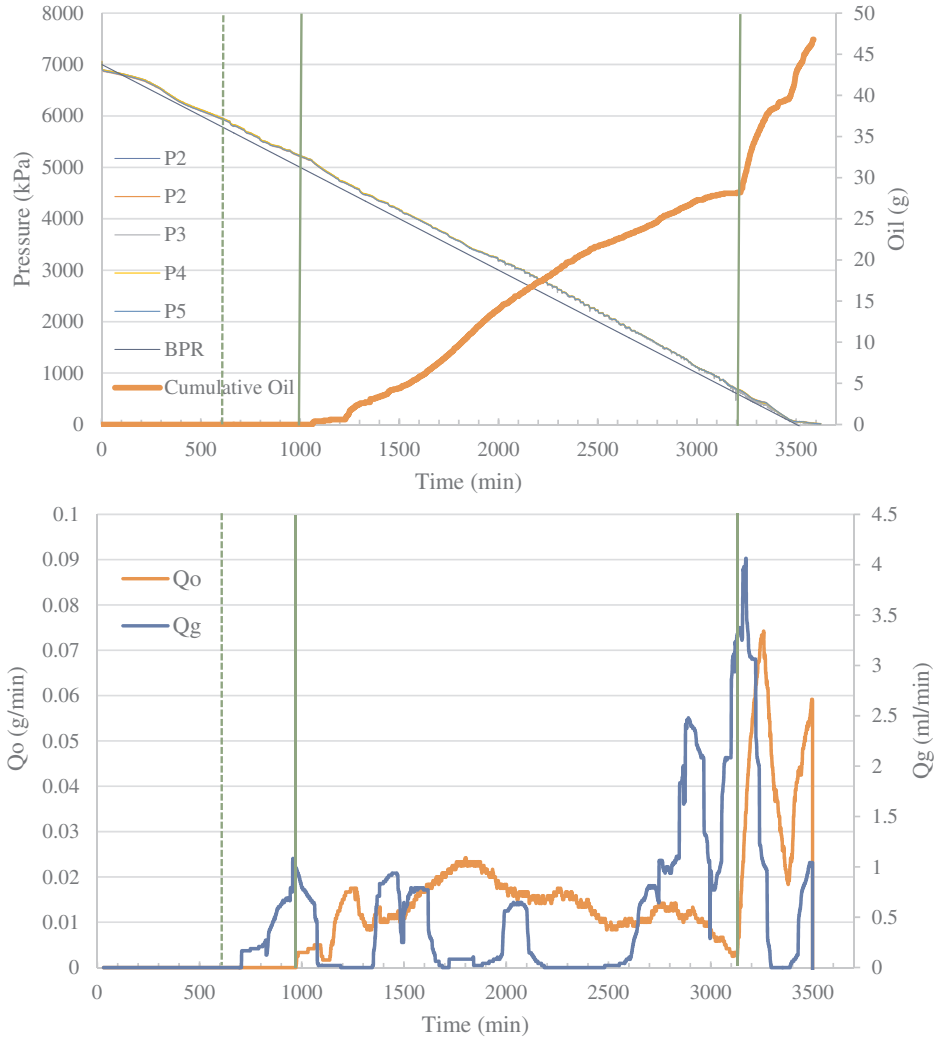

Fig. 7. Cumulative oil production, Oil/Gas Production Rate, and the Inner Pressure Curves with Pressure Decline Rater of 2 kPa/min.

stage of the normal solution gas drive, the maximum oil production per unit pressure depletion is about 0.0625 g/kPa. (10 kg/ MPa). At this normal solution gas drive stage, experiments with pressure decline rates of 2 and 8 kPa/min produced 28.8 g and 32.8 g of oil, respectively. For the test with the pressure decline rate of 2 kPa/min, since there is a gas single-phase flow region in the early stage of the normal solution gas drive region, and if the effect of the foamy oil is removed, there would be minimal production difference in the normal solution gas drive region. From this, the limit of oil production from normal solution gas drive is approximately 30 g.

When this experiment runs to 13 h, and the pressure drops to about 600 kPa, a sudden increase in oil production rate exists. The characteristics of this foamy oil flow region are similar to those of the pressure decline rate of 2 kPa/min. In the experiment with a pressure decline rate of 2 kPa/min, the oil production curve fluctuates, indicating that the foamy oil produced is unstable. The oil production in the foamy oil flow region is 18.6 g. However, in the experiment with a pressure decline rate of 8 kPa/min, the oil production curve is very smooth, indicating that the foamy oil produced is stable. Here the oil production in the foamy oil flow region is 27.5 g. This shows that compared to the pressure decline rate of 2 kPa/min, the pressure decline rate of 8 kPa/min can produce a more stable foamy oil flow.

3.2.1.3. Pressure decline rate: 16 kPa/min. Fig. 9 shows the cumulative oil production curve and the inner pressure curves as a function of time elapsed in the experiment with a pressure decline rate of 16 kPa/min. When the pressure is higher than the bubble point, the oil production and gas production characteristics are the same as the experiment with a pressure decline rate of 8 kPa/min. However, when the pressure drops below the bubble point pressure, nitrogen begins to be released from the oil. In this stage, the oil and gas production rate are very low since the nitrogen bubbles are trapped in the high viscosity oil and the bubble size is so small that it is negligible. Despite of this low production rate, the gas molecules start to nucleate.

When this experiment runs to 4.6 h, and the pressure drops to about 2,600 kPa, there is a sudden increase in oil production rate. From here on, foamy oil begins to produce. In this region, small bubbles begin to aggregate toward the nucleated bubbles and form a slightly larger bubble before they are separated from the oil. In this foamy oil flow region, a total of 66.2 g of oil is produced. It can be seen from Fig. 9 that the gas production characteristics at this stage are very consistent with the production characteristics of the foamy oil. This stage is maintained until the pressure at the outlet port of the sand-pack model drops to atmospheric pressure.

When the pressure at the outlet of the model drops to atmospheric pressure, there is still some pressure inside the model. This shows that the previously dissolved nitrogen has not been completely released from the oil, and the remaining small amount of nitrogen is still being released slowly. However, since only a small amount of nitrogen remains, and the gas release rate is very slow, it is insufficient to form foamy oil flow. This stage is mainly dominated by normal solution gas drive, and it lasts nearly two-thirds of the total production time with a

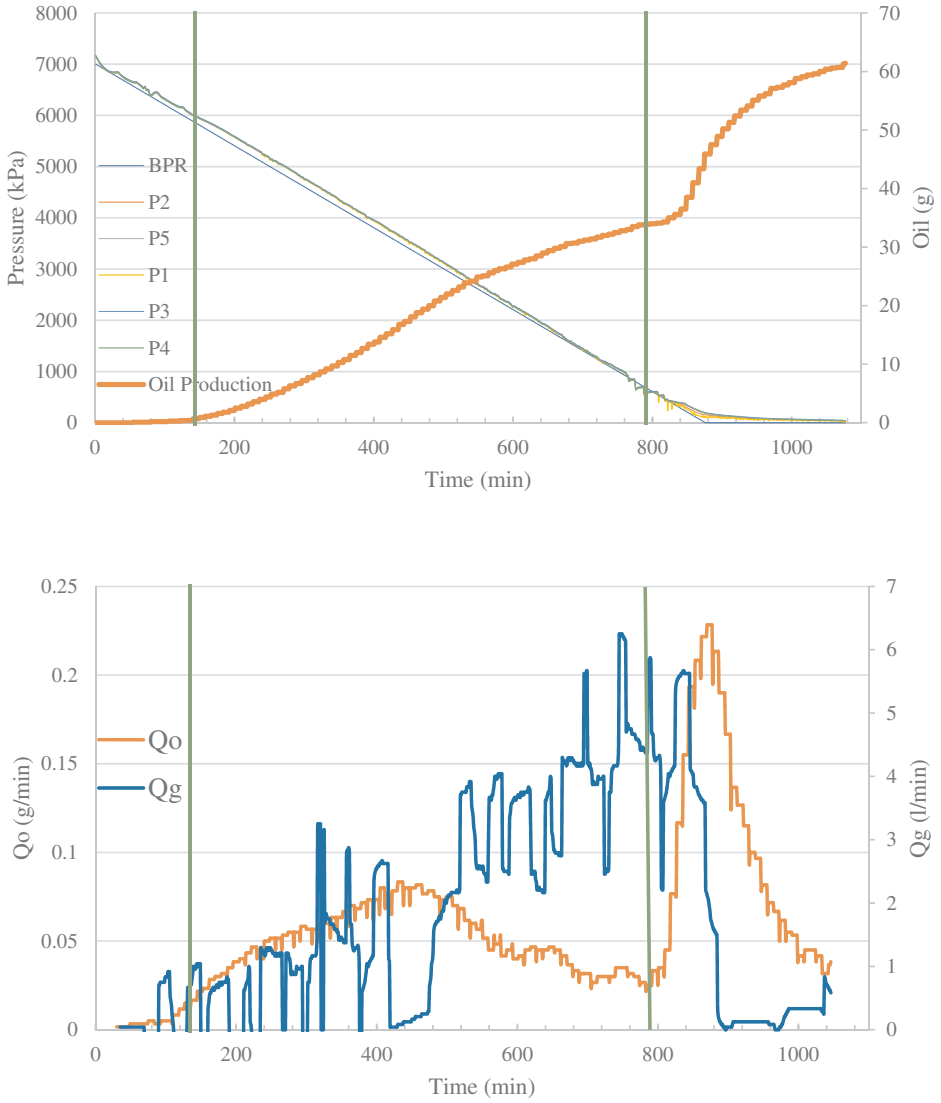

Fig. 8. Cumulative oil production, Oil/Gas Production Rate, and the Inner Pressure Curves with Pressure Decline Rater of 8 kPa/min.

total production of 23 g of oil.

3.2.1.4. Pressure decline rate: 32 kPa/min. The production curve characteristic of the experiment with a pressure decline rate of 32 kPa/min is very similar to the pressure decline rate of 16 kPa/min. The difference being more oil is produced during the foamy oil flow region (71.6 g). As the pressure decline rate increases, more nitrogen remains in the oil after the end of the foamy oil flow region (Fig. 10). This allows the normal solution gas drive to be maintained for a longer period of time and produces more oil (45.6 g).

Table 7 shows the oil recovery factor of each part of the flow region in each of the four experiments. The oil production of single-phase flow is too small to discover any trends. The causes of normal solution gas drive in the low pressure decline rates differ from the causes of normal solution gas drive in the high pressure decline rates. In the normal solution gas drive region, there is a tendency for the recovery factor to increase as the pressure decline rate increases. In the foamy oil flow region, as the pressure decline rate increases, the oil recovery rate increases significantly. This shows that the higher the pressure decline rate, the stronger the foamy oil can be formed.

3.2.2. Pressure analysis

In this study, the pressure data is more reflective for the characteristics of the flow state. The distribution of pressure points is shown in Fig. 11. This section will include four experiments that compare the difference in pressure between P5-P1, P5-P2, P5-P3, and P5-P4, and analyze the pressure changes in the various flow regions. The pressure transducer at P1 shows the pressure at the outlet port outside the model, which is also the pressure of the BPR. The pressure transducers from P2 to P5 shows the pressure of the four ports in the model, which are evenly distributed from the outlet port to the inlet port.

3.2.2.1. Pressure decline rate: 2 kPa/min. The change in pressure difference with time is shown in Fig. 12. In the single-phase flow region, whether it is the oil single-phase flow of the former part or the gas single-phase flow of the latter part, the pressure difference of the five pressure points is less than 15 kPa. The error of the pressure transducers are ± 5 kPa, so the pressure differences between five pressure points are very small. Since there is no pressure difference in the entire one-dimensional model, there is no oil production at this stage.

When the normal solution gas drive region starts, the pressure difference inside the model begins to rise gradually. There has been a significant increase in pressure difference starting from the middle of this region. From the curves of oil and gas production, the oil

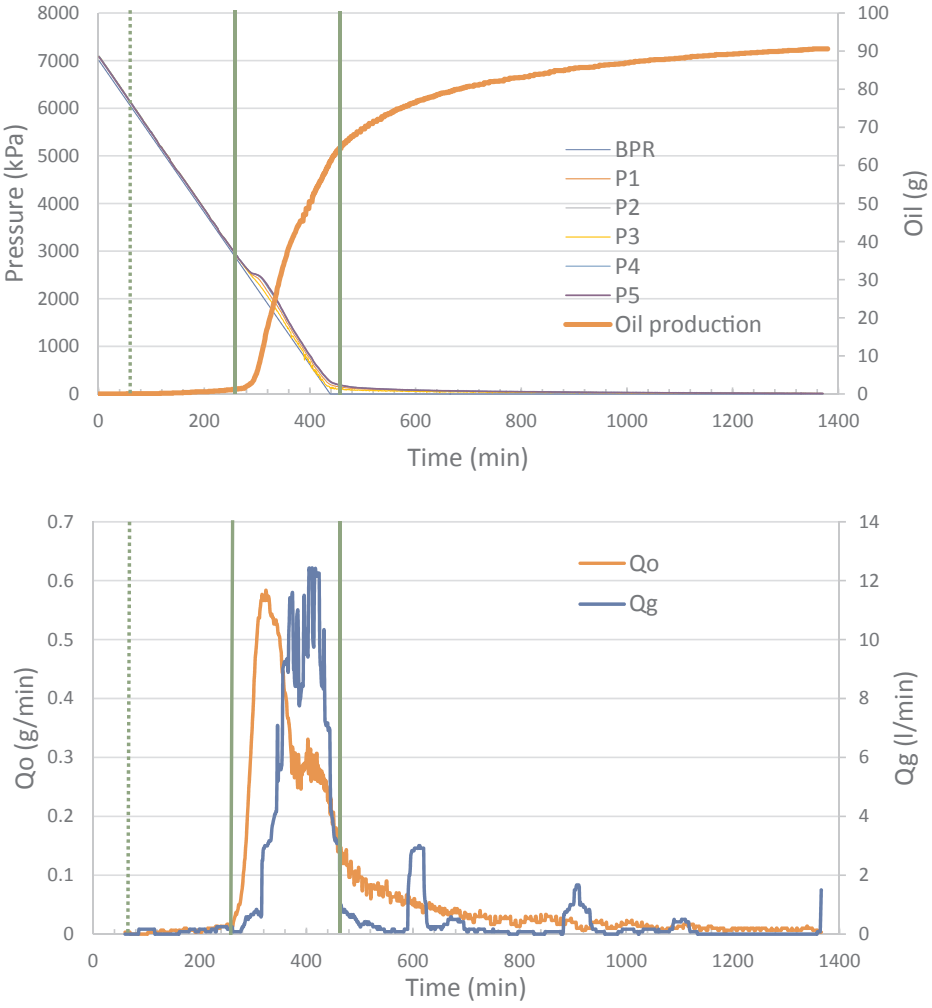

Fig. 9. Cumulative oil production, Oil/Gas Production Rate, and the Inner Pressure Curves with Pressure Decline Rater of 16 kPa/min.

production rate is slowly reduced after this point, while the gas production rate is suddenly increased. This shows that the change in pressure difference after the mid stage is caused by a large amount of gas production.

When the pressure difference rises to a certain extent, or when the volume of the bubble trapped in the oil is increased to a certain extent, it enters the stage of foamy oil production. At the start of the foamy oil flow stage, the pressure difference begins to rise sharply, indicating that the model fluid volume changes significantly and continue to increase.

Combined with changes in pressure and changes in previous oil/gas production trends, a reasonable explanation can be given for the foamy oil generation at this stage. The gas release rate of nitrogen from the oil is defined as the following formula;

$$v_{release} = \frac{dV}{dP} \times \frac{dP}{dt} \times \frac{ZTP_{sc}}{z_{sc} T_{sc} P} \tag{4.4}$$

$$\frac{dV}{dP} = A \times \frac{dS}{dP} \tag{4.5}$$

where $v_{release}$ is the gas release rate of nitrogen from the oil; V is the gas volume under standard condition; P is the pressure; t is the time; Z is the compressibility factor; T is the temperature; A is a coefficient that determines how much gas is actually released from the oil, which is mainly related to the pressure fluctuations diffusion coefficient; S is the solubility.

The solubility of nitrogen in this oil sample is determined in PVT tests. In theory, when the time is long enough, $\frac{dV}{dP}$ equals $\frac{dS}{dP}$. In this study, assuming that $\frac{dV}{dP}$ equals $\frac{dS}{dP}$. Due to the significant gas compression coefficient, the volumetric rate at low pressure is greater than the volumetric rate at high pressure. At the pressure decline rate of 2 kPa/min, the pressure at the beginning of the normal solution gas drive and at the beginning of the foamy oil flow are 5241 kPa and 303 kPa, respectively. The gas release rate of nitrogen at these two points is 0.031 l/m^3·min and 0.528 l/m^3·min, respectively. For that reason, when the gas release rate of nitrogen exceeds 0.031 l/m^3·min, normal solution gas drive occurs, and when the gas release rate of nitrogen exceeds 0.528 l/m^3·min, foamy oil flow is dominant.

3.2.2.2. Pressure decline rate: 8 kPa/min. The pressure differences curves with a pressure decline rate of 8 kPa/min are very similar to the curves of the previous experiment. The difference is that the curves at 8 kPa/min are more stable during both the normal solution gas drive region and the foamy oil flow region. The same method is used to calculate the volumetric rate of nitrogen released per unit volume of oil. At the pressure decline rate of 8 kPa/min, the pressure at the beginning of the normal solution gas drive and at the beginning of the foamy oil flow is 6,000 kPa and 695 kPa, respectively. The volumetric rate of nitrogen released at these two points is 0.107 l/m^3·min and 0.920 l/m^3·min, respectively. This shows that a higher volumetric rate of nitrogen released (or a higher pressure decline rate) results in a more stable normal solution gas drive and foamy oil flow (Fig. 13).

3.2.2.3. Pressure decline rate: 16 kPa/min and 32 kPa/min. In these experiments, the foamy oil flow region follows the single-phase flow

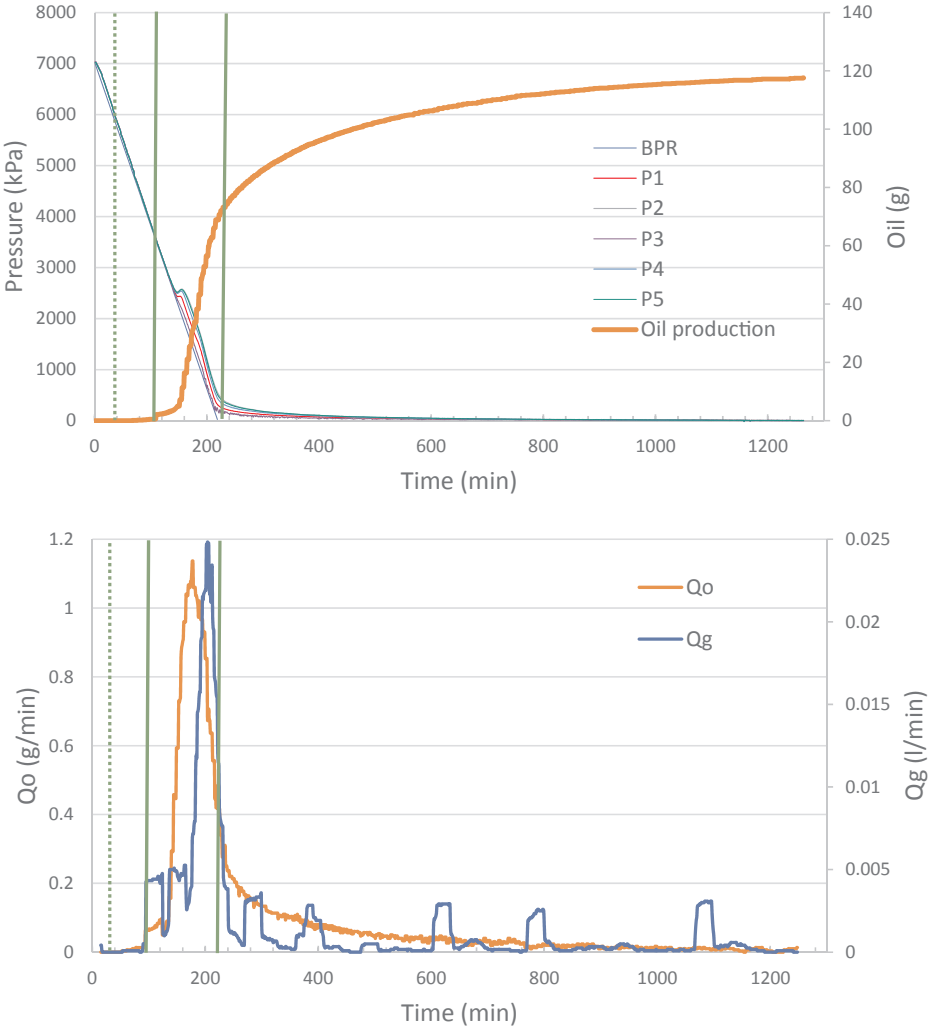

Fig. 10. Cumulative oil production, Oil/Gas Production Rate, and the Inner Pressure Curves with Pressure Decline Rater of 32 kPa/min.

Table 7
Oil Recovery Factor of Each Experiment.

Pressure Decline Rate, kPa/min	Oil Recovery Factor, %			
	Single-Phase Flow	Normal solution gas drive	Foamy oil flow	Total
2	0.00	7.76	5.12	12.88
8	0.11	9.22	7.57	16.90
16	0.39	6.33	18.22	24.94
32	0.11	12.55	19.71	32.37

region. The pressure at the starting point of the foamy oil flow region for these two experiments is 2,525 kPa and 3,720 kPa, respectively. The corresponding volumetric rate of nitrogen released is 0.507 l/m^3·min and 0.698 l/m^3·min, respectively. Higher volumetric rate results in a more stable foamy oil flow for the experiment with the pressure decline rate of 32 kPa/min (as shown in Fig. 14). Since the starting point of the normal solution gas drive region is after the BPR pressure drops to atmospheric pressure, the actual pressure decline rate in the model starts to differ and cannot be measured. Therefore, the gas release rate at the beginning of the normal solution gas drive region of these two experiments cannot be calculated.

Table 8 shows the volumetric rate of nitrogen released per unit volume of oil at the beginning of each flow region in these four experiments. The condition at which the normal solution gas drive started is 0.031 l/m 3 ·min, which is determined by experiment under pressure decline rate of 2 kPa/min, because the experiment with the pressure decline rate of 2 kPa/min experiences a period between gas single-phase flow and normal solution gas drive. In the experiment with the pressure decline rate of 8 kPa/min, the pressure decline rate is faster than the start limits of normal solution gas drive. When the pressure drops to the bubble point pressure, normal solution gas drive begins immediately. Moreover, the condition at which the foamy oil flow started is around 0.52–0.9 l/m^3 ·min.

3.2.3. Comparison with other solvent

The four sets of curves in Fig. 15 are the production curves for the pressure depletion tests in the same 1-D sand-pack model for carbon dioxide, methane, methane-propane mixture, and propane, respectively. These curves are from Xiang's and Mingyi's studies [37,51].

The production curves of the experiments for carbon dioxide, methane and methane-propane mixture are very similar to those of nitrogen experiments. Moreover, each inflection point in the curves of the two groups of experiments can be clearly explained by the viewpoint of the gas release rate.

George et al. studied the effects of oil viscosity on formation of foamy oil and found that the stability of bubbles is highly dependent on oil viscosity [7]. The results in this study shows that, the stability of foamy oil flow also affected by the gas release rate [52].

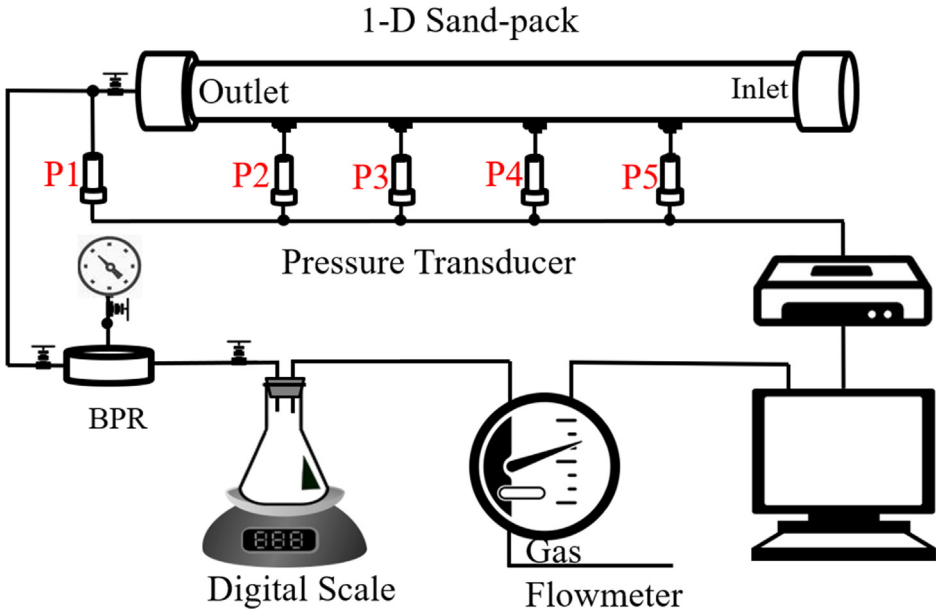

Fig. 11. The Distribution of Pressure Points.

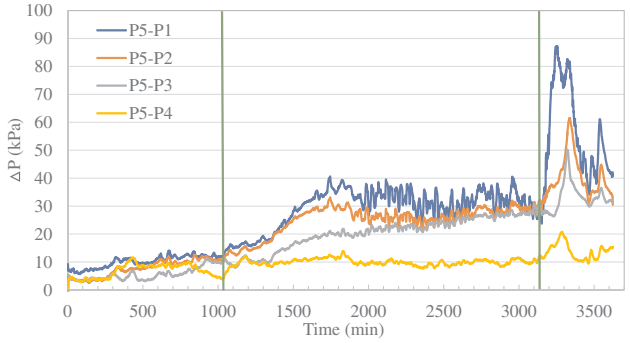

Fig. 12. Pressure Difference in the Test with Pressure Decline Rate of 2 kPa/min.

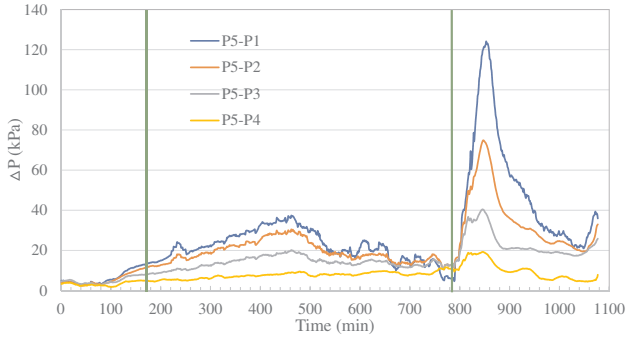

Fig. 13. Pressure Difference in the Test with Pressure Decline Rate of 8 kPa/min.

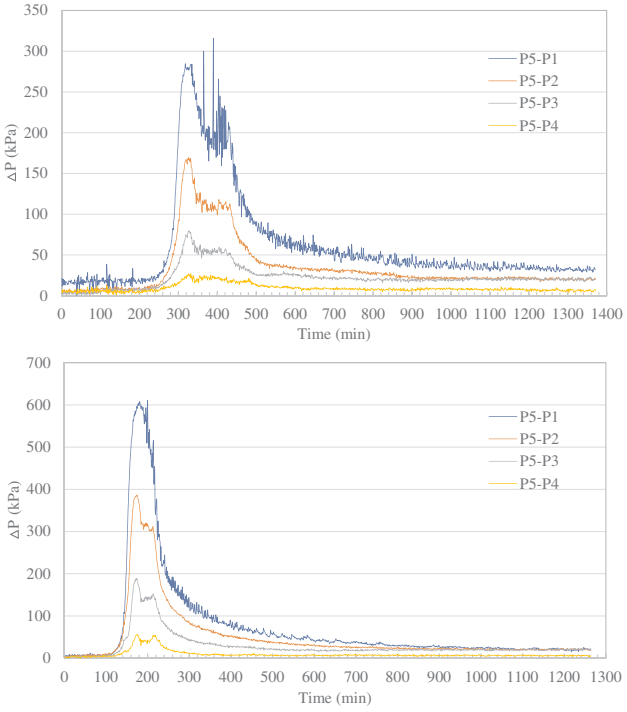

Fig. 14. Pressure Difference in the Test with Pressure Decline Rate of 16 and 32 kPa/min.

4. Conclusions

Since foamy oil is a very significant production mechanism in huff-n-puff, especially in Cyclic Solvent Injection, the objective of this chapter is to experimentally determine whether or not the oil saturated with nitrogen can form foamy oil during the pressure depletion process. This chapter has reached the following conclusions in the experiments of nitrogen live oil pressure depletion tests.

The solubility of nitrogen is low and does not have much effect on

Table 8
Nitrogen Release Rate at Each Stage.

Pressure decline rate, kPa/min	Pressure at Starting Point, kPa		Gas Release Rate at Starting Point, l/m^3·min	
	Normal solution gas drive	Foamy oil flow	Normal solution gas drive	Foamy oil flow
2	5242	303	0.031	0.528
8	6000	695	0.107	0.920
16		2525		0.507
32		3670		0.698

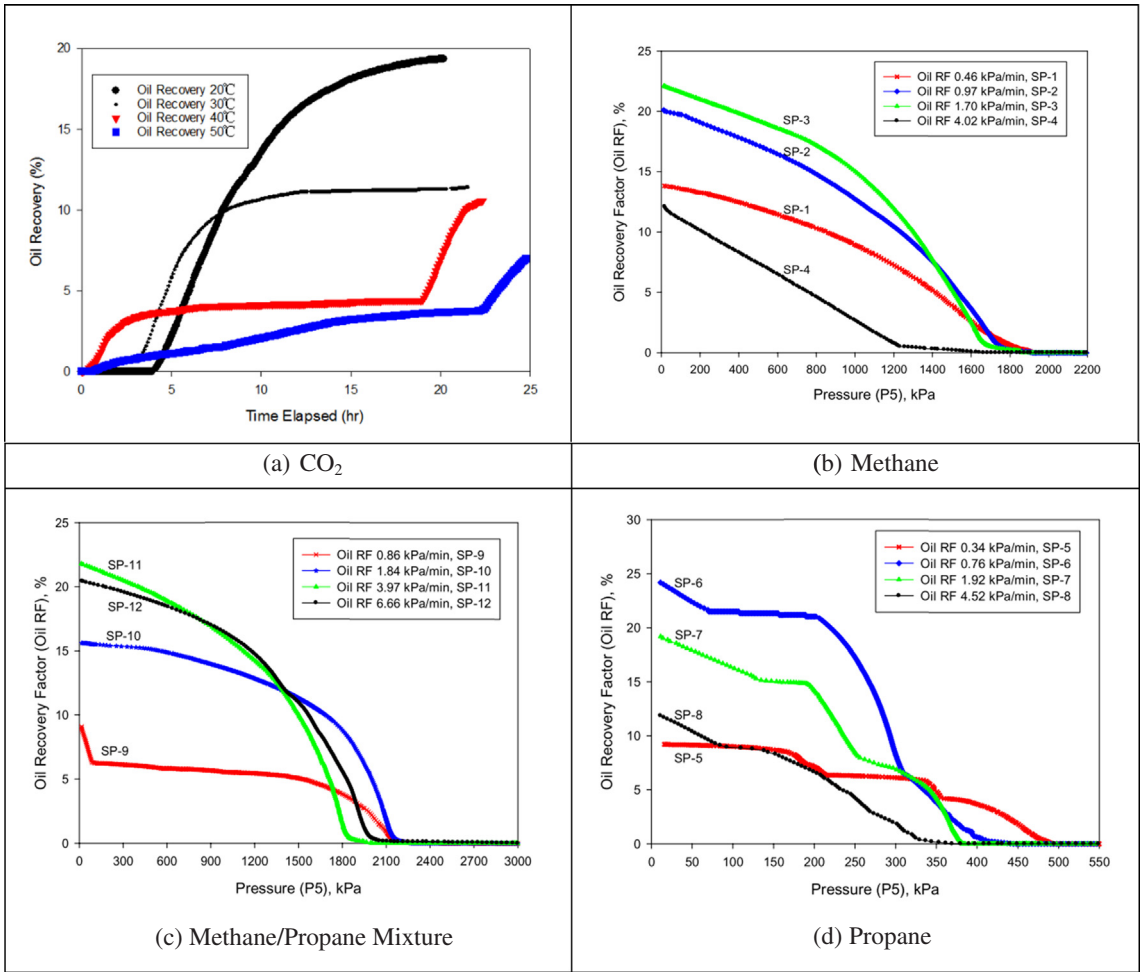

Fig. 15. Production Curves for Other Solvents [37,51].

viscosity reduction under high temperature.

The higher the pressure decline rate, the greater the oil recovery factor and the smaller the gas recovery factor.

In the normal solution gas drive region, the two groups of experiments (one with low pressure decline rates and the other with high pressure decline rates) have different causes of normal solution gas drive. Under low pressure decline rate, the pressure decline rate does not affect the oil recovery factor of the normal solution gas drive stage. The maximum oil production per unit pressure depletion is about 0.01 g/kPa. Under high-pressure decline rate, due to the difference in the amount of residual gas in the oil from the previous foamy oil flow stage, the faster the pressure decline rate, the higher the oil recovery factor in the normal solution gas drive region.

Under the premise that the viscosity of the oil and formation conditions remain unchanged, the change of the flow state mainly depends on the volumetric rate of the gas release. With the increase of gas release rate, the flow state is followed by gas single-phase flow, normal solution gas drive, and foamy oil flow.

In the foamy oil flow stage, as the pressure decline rate increases, the oil recovery rate also increases significantly. This shows that the higher the pressure decline rate, the stronger the foamy oil can be formed.

It is finally confirmed that in the high-pressure reservoir at 50 °C, the nitrogen-heavy oil live oil in pressure decline tests can form foamy oil.

Declaration of Competing Interest

The authors declare that they have no known competing financial interests or personal relationships that could have appeared to influence the work reported in this paper.

Acknowledgments

The authors would like to acknowledge the financial support from the Open Fund (PLN201803) of State Key Laboratory of Oil and Gas Reservoir Geology and Exploitation (Southwest Petroleum University), and National Natural Science Foundation of China (Grant No:51704245). The authors gratefully thank the anonymous reviewers for their constructive and valuable comments.

References

[1] Ahadi A, Torabi F. Effect of light hydrocarbon solvents on the performance of CO2-based cyclic solvent injection (CSI) in heavy oil systems. J Petrol Sci Eng 2018;163:526–37. https://doi.org/10.1016/j.petrol.2017.12.062.

[2] Bai J, Liu H, Wang J, Qian G, Peng Y, Gao Y, et al. CO2, water and N2 injection for enhanced oil recovery with spatial arrangement of fractures in tight-oil reservoirs using huff-'n-puff. Energies 2019;12(5):1–29. https://doi.org/10.3390/en12050823.

[3] Bozorg M, Addis B, Piccialli V, Ramírez-Santos ÁA, Castel C, Pinnau I, et al. Polymeric membrane materials for nitrogen production from air: A process synthesis study. Chem Eng Sci 2019;207:1196–213. https://doi.org/10.1016/j.ces.2019.07.029.

[4] Campo MC, Magalhães FD, Mendes A. Separation of nitrogen from air by carbon molecular sieve membranes. J Membr Sci 2010;350(1–2):139–47. https://doi.org/10.1016/j.memsci.2009.12.021.

[5] Crandall GR, Wise TH. Market Outlook for Canadian Heavy Crude. J Can Pet Technol 1984;23(3):67–71.
[6] Feng T, Wu Y, Hu C, Gong Y, Song Y. Technology of fire flooding process control: Application to fire flooding in a deep and thick heavy oil reservoir in China. Society of Petroleum Engineers – SPE Asia Pacific Oil and Gas Conference and Exhibition 2018, APOGCE 2018. 2018.
[7] George DS, Hayat O, Kovscek AR. A microvisual study of solution-gas-drive mechanisms in viscous oils. J Petrol Sci Eng 2005;46(1–2):101–19. https://doi.org/10.1016/j.petrol.2004.08.003.
[8] Huang T, Zhou X, Yang H, Liao G, Zeng F. CO 2 flooding strategy to enhance heavy oil recovery. Petroleum 2017;3(1):68–78. https://doi.org/10.1016/j.petlm.2016.11.005.
[9] Jia X, Zeng F, Gu Y. Dynamic solvent process (DSP) for enhancing heavy oil recovery. Can J Chem Eng 2015;93(5):832–41. https://doi.org/10.1002/cjce.22178.
[10] Jin F-Y, Gao H, Chen Y-F, Wei B, Li Y-B, Dong H, et al. Low temperature oxidation characteristics analysis of ultra-heavy oil by thermal methods. J Ind Eng Chem 2017;48:249–58. https://doi.org/10.1016/j.jiec.2017.01.017.
[11] Jiuquan A, Ji L, Technology P, Co O. Steamflood Trial and Research on Mid-deep Heavy-Oil Reservoir QI40 Block in Liaohe Oilfield. SPE International Oil & Gas Conference. 2006.
[12] Knorr KD, Imran M. Solvent-chamber development in 3D-physical-model experiments of solvent- Vapour extraction (SVX) processes with various permeabilities and solvent-vapour qualities. J Can Pet Technol 2012;51(6):425–36. https://doi.org/10.2118/149190-PA.
[13] Lang JE. Performance of Elk Basin Tensleep reservoir with nitrogen injection. Drilling and Production Practice 1954;1954:90–8.
[14] Li L, Su Y, Hao Y, Zhan S, Lv Y, Zhao Q, et al. A comparative study of CO2 and N2 huff-n-puff EOR performance in shale oil production. J Petrol Sci Eng 2019;181. https://doi.org/10.1016/j.petrol.2019.06.038.
[15] Lin J, Ren T, Cheng Y, Nemcik J, Wang G. Cyclic N2 injection for enhanced coal seam gas recovery: A laboratory study. Energy 2019;188:116115https://doi.org/10.1016/j.energy.2019.116115.
[16] Lin L, Ma H, Zeng F, Gu Y. A Critical Review of the Solvent-Based Heavy Oil Recovery Methods. SPE Heavy Oil Conference-Canada 2014;1–20. https://doi.org/10.2118/170098-MS.
[17] Lu T, Li Z, Li J, Hou D, Zhang D. Flow behavior of N2 huff and puff process for enhanced oil recovery in tight oil reservoirs. Sci Rep 2017;7(1):1–14. https://doi.org/10.1038/s41598-017-15913-5.
[18] Maini BB. Foamy-Oil Flow. J Petrol Technol 2001;53(10):54–64. https://doi.org/10.2118/68885-JPT.
[19] Maini BB, Sarma HK, George AE. Significance of Foamy-oil Behaviour In Primary Production of Heavy Oils. J Can Pet Technol 2010;32(09). https://doi.org/10.2118/93-09-07.
[20] Mansourizadeh A, Ismail AF. Hollow fiber gas-liquid membrane contactors for acid gas capture: A review. J Hazard Mater 2009;171(1–3):38–53. https://doi.org/10.1016/j.jhazmat.2009.06.026.
[21] Mehrotra AK, Svrcek WY. Correlations for properties of bitumen with CO2, CH4 and N2 and experiments with combustion gas mixtures. J Can Pet Technol 1982;21(6):95–104.
[22] Miller BJ, Hamilton-Smith T. Field case: Cyclic gas recovery for light oil-using carbon dioxide/nitrogen/natural gas. Proceedings – SPE Annual Technical Conference and Exhibition, 1999-Septe. 1998. p. 501–7.
[23] Nelson DG, Sheehy P, O'Donnell J, Heisler MA. Saving Heavy Oil Reserve Value in a Carbon Constrained Market. SPE Western Regional Meeting 2016;32(Ab 32). https://doi.org/10.2118/180447-ms.
[24] Nguyen P, Carey JW, Viswanathan HS, Porter M. Effectiveness of supercritical-CO2 and N2 huff-and-puff methods of enhanced oil recovery in shale fracture networks using microfluidic experiments. Appl Energy 2018;230:160–74. https://doi.org/10.1016/j.apenergy.2018.08.098.
[25] Rangriz Shokri A, Babadagli T. Feasibility assessment of heavy-oil recovery by CO2 injection after cold production with sands: Lab-to-field scale modeling considering non-equilibrium foamy oil behavior. Appl Energy 2017;205:615–25. https://doi.org/10.1016/j.apenergy.2017.08.029.
[26] Sheng JJ, Maini BB, Hayes RE, Tortike WS. Critical Review of Foamy Oil Flow, Transport in Porous Media. Transp Porous Media 1999;35(4):157–87.
[27] Shi L, Liu P, Shen D, Liu P, Xi C, Zhang Y. Improving heavy oil recovery using a top-driving, CO2-assisted hot-water flooding method in deep and pressure-depleted reservoirs. J Petrol Sci Eng 2019;173:922–31. https://doi.org/10.1016/j.petrol.2018.10.088.
[28] Sinanan B, Budri M. Nitrogen injection application for oil recovery in Trinidad. Society of Petroleum Engineers – SPETT Energy Conference and Exhibition 2012. 2012. p. 42–52. doi: 10.2118/156924-ms.
[29] Smith GE. Fluid Flow and Sand Production in Heavy-Oil Reservoirs Under Solution-Gas Drive. SPE Prod Eng 1988;3(02):169–80. https://doi.org/10.2118/15094-PA.
[30] Sun Y, Wu Q, Wei M, Bai B, Ma Y. Experimental study of friction reducer flows in microfracture. Fuel 2014;131:28–35. https://doi.org/10.1016/j.fuel.2014.04.050.
[31] Tao L, Li Z, Bi Y, Li B, Zhang J. Multi-combination exploiting technique of ultra-heavy oil reservoirs with deep and thin layers in Shengli Oilfield. Pet Explor Dev 2010;37(6):732–6. https://doi.org/10.1016/S1876-3804(11)60007-4.
[32] Thomas LK, Dixon TN, Pierson RG, Hermansen H. Ekofisk nitrogen injection. SPE Form Eval 1991;6(2):151–60. https://doi.org/10.2118/19839-PA.
[33] Wang C, Zhong L, Li J, Chen G, Zang Y, Wei F. Laboratory study on steam and nitrogen co-injection for mid-deep heavy oil reservoirs. Society of Petroleum Engineers - SPE Kuwait Oil and Gas Show and Conference. 2015.
[34] Wang Haiwen, Yang D. Reliability improvement of progressive cavity pump in a deep heavy oil reservoir. Society of Petroleum Engineers - Progressing Cavity Pumps Conference 2010. 2010. p. 106–12.
[35] Wang Hongyang, Zeng F, Zhou X. Study of the Non-Equilibrium PVT Properties of Methane- and Propane-Heavy Oil Systems. SPE Heavy Oil Conference - Canada 2015;2015:1–23. https://doi.org/10.2118/174498-MS.
[36] Wang X, Peng X, Zhang S, Du Z, Zeng F. Characteristics of oil distributions in forced and spontaneous imbibition of tight oil reservoir. Fuel 2018;224:280–8. https://doi.org/10.1016/j.fuel.2018.03.104.
[37] Wu M. Effects of Temperature and Heavy Oil Viscosity on Foamy Oil Flow in Porous Media. M.Sc: Thesis, University of Regina; 2018.
[38] Wuensche R. Nitrogen injection for enhanced oil recovery. Annual Technical Meeting, PETSOC ATM 1978. 1978. (78). Doi: 10.2118/78-29-44.
[39] Yadali Jamaloei B, Dong M, Yang P, Yang D, Mahinpey N. Impact of solvent type and injection sequence on Enhanced Cyclic Solvent Process (ECSP) for thin heavy oil reservoirs. J Petrol Sci Eng 2013;110:169–83. https://doi.org/10.1016/j.petrol.2013.08.028.
[40] Yazdani A, Maini BB. Effect of Height and Grain Size on the Production Rates in the Vapex Process: Experimental Study. SPE Reservoir Eval Eng 2006;8(03):205–13. https://doi.org/10.2118/89409-pa.
[41] Yu W, Lashgari H, Sepehrnoori K. Simulation Study of CO2 Huff-n-Puff Process in Bakken Tight Oil Reservoirs. SPE Western North American and Rocky Mountain Joint Regional Meeting, 2(April). 2014.
[42] Yu Y, Sheng JJ. An experimental investigation of the effect of pressure depletion rate on oil recovery from shale cores by cyclic N2 injection. Society of Petroleum Engineers - Unconventional Resources Technology Conference, URTeC 2015. 2015.
[43] Yue P, Xie Z, Huang S, Liu H, Liang SB, Chen X. The application of N2 huff and puff for IOR in fracture-vuggy carbonate reservoir. Fuel 2018;234:1507–17. https://doi.org/10.1016/j.fuel.2018.07.128.
[44] Zhang K, Zhou X, Peng X, Zeng F. A comparison study between N-Solv method and cyclic hot solvent injection (CHSI) method. J Petrol Sci Eng 2019;173:258–68. https://doi.org/10.1016/j.petrol.2018.09.061.
[45] Zhang Y. Effects of Temperature on Foamy Oil Flow in Solution Gas-Drive in Cold Lake Field. J Can Petrol Technol 1999(10). https://doi.org/10.1007/s10973-014-3688-4.
[46] Zhao Y long, Xie S chang, Peng X long, Zhang L hui. Transient pressure response of fractured horizontal wells in tight gas reservoirs with arbitrary shapes by the boundary element method. Environmental Earth Sciences 2016;75(17):1–14. https://doi.org/10.1007/s12665-016-6013-7.
[47] Zhou X, Yuan Q, Peng X, Zeng F, Zhang L. A critical review of the CO2 huff 'n' puff process for enhanced heavy oil recovery. Fuel 2018;215:813–24. https://doi.org/10.1016/j.fuel.2017.11.092.
[48] Zhou X, Yuan Q, Rui Z, Wang H, Feng J, Zhang L, et al. Feasibility study of CO2 huff 'n' puff process to enhance heavy oil recovery via long core experiments. Appl Energy 2019;236:526–39. https://doi.org/10.1016/j.apenergy.2018.12.007.
[49] Zhou X, Jiang Q, Zhang L, Feng J, Chu B, Zeng F, et al. Determining CO_2 diffusion coefficient in heavy oil in bulk phase and in porous media using experimental and mathematical modeling methods. Fuel 2019:116205https://doi.org/10.1016/j.fuel.2019.116205.
[50] Zhou X, Zeng F, Zhang L. Improving Steam-Assisted Gravity Drainage performance in oil sands with a top water zone using polymer injection and the fishbone well pattern. Fuel 2016;184:449–65. https://doi.org/10.1016/j.fuel.2016.07.040.
[51] Zhou X, Zeng F, Zhang L, Wang H. Foamy oil flow in heavy oil-solvent systems tested by pressure depletion in a sandpack. Fuel 2016;171:210–23. https://doi.org/10.1016/j.fuel.2015.12.070.
[52] Zhou X, Zeng F, Zhang L, Jiang Q, Yuan Q, Wang J, et al. Experimental and mathematical modeling studies on foamy oil stability using a heavy oil–CO_2 system under reservoir conditions. Fuel 2020;264:116771https://doi.org/10.1016/j.fuel.2019.116771.